



Phosphate recovery from aqueous solution by K-zeolite synthesized from fly ash for subsequent valorisation as slow release fertilizer

Mehrez Hermassi^{a,c,*}, Cesar Valderrama^b, Oriol Font^d, Natalia Moreno^d, Xavier Querol^d, Narjès Harrouch Batis^c, Jose Luis Cortina^{b,e}

^a Cranfield Water Science Institute, Vincent Building, Cranfield University, Bedfordshire MK43 0AL, UK

^b Chemical Engineering Department, Barcelona Research Center for Multiscale Science and Engineering Escola d'Enginyeria de Barcelona Est (EEBE), Universitat Politècnica de Catalunya (UPC)-BarcelonaTECH, C/ Eduard Maristany 10-14, Campus Diagonal-Besòs, 08930 Barcelona, Spain.

^c Dept. Biol. Chem. Eng., National Institute of Applied Sciences and Technology (INSAT), University of Carthage (, Tunisia)

^d Environmental Geochemistry and Atmospheric Research Group (EGAR), Institute of Environmental Assessment and Water Research—Severo Ochoa Excellence Center (IDAEA), Spanish Council of Scientific Research (CSIC), Jordi Girona 18-26, 08034 Barcelona, Spain

^e CETAqua, Carretera d'Esplugues 75, 08940 Cornellà de Llobregat, Spain

ARTICLE INFO

Article history:

Received 17 February 2020

Received in revised form 13 April 2020

Accepted 24 April 2020

Available online xxx

Editor: Damia Barcelo

Keywords

Potassium zeolite

Fly ash

Phosphate recovery

Treated wastewater

Sorption

Brushite

ABSTRACT

The sorption of phosphate by K-zeolites synthesized from fly ash (FA) by hydrothermal conversion is investigated in this study. The aim is the synthesis of Ca bearing K-zeolites to recover phosphate from urban and industrial wastewater effluents. The loaded zeolites are considered as a by-products rich in essential nutrients such K and P (KP1) with a potential use as slow release fertilizer. A number of synthesis conditions (temperature, KOH-solution/FA ratio, KOH concentration, and activation time) were applied on two FA samples (FA-TE and FA-LB) with similar glass content but different content of crystalline phases, to optimize the synthesis of a zeolitic sorbent suitable for the subsequent phosphate uptake. Merlinoite and W rich zeolitic products synthesized from FA-LB and FA-TE were found to have sorption properties for phosphate removal. A maximum phosphate sorption capacity of 250 mgP-PO₄/g and 142 mgP-PO₄/g for the zeolitic products selected (KP1-LB and KP1-TE, respectively) was achieved. The dominant phosphate sorption mechanism, in the pH range (6–9) of treated wastewater effluents, indicated that sorption proceeds via a diffusion-controlled process involving phosphate ions coupled with calcium supply dissolution from K-zeolitic products and subsequent formation of brushite (CaHPO₄·2H₂O(s)). The phosphate loaded sorbent containing a relatively soluble phosphate mineral is appropriate for its use as a synthetic slow release fertilizer. The simultaneous valorisation of fly ash waste and the P recovery from treated wastewaters effluents, (a nutrient with scarce natural resources and low supply) by obtaining a product with high potential for land restoration and agriculture will contribute to develop one example of circularity.

© 2020

1. Introduction

Demand for industrial products has grown considerably in recent years, along with energy consumption. While growth in energy consumption has been driven largely by an ongoing long-term trend, despite raising the residues generated by intensive industry subsectors (i.e. chemicals, iron and steel, cement, pulp and paper and aluminium) (International Energy Agency, IEA, 2019). To reduce the generation of industrial residues and the unproductive and high cost of landfilling, since 2016 the European Commission (EC) has adopted the EU

Circular Economy Action Plan (European Commission, 2018) to promote the transition to a more efficient economy, with the aim to contribute to “closing the loop” of product lifecycles through better and larger recycling and re-use, bringing environmental, economic, and social benefits. In this sense, it is worth noting the coal power plants for the generation of electricity and the fertilizer industry, two important sectors contributing to the consumption of resources and the generation of waste.

Despite coal's share in primary energy fell in advanced economies, coal is still being the main source of electricity in the world (38%) (Wang et al., 2020). The coal production and demand worldwide grew by 3.3% and 2% in 2018, respectively and primarily driven by China, India and Indonesia, while fell in Europe and North America (Wang et al., 2020). The generation of coal fly ash worldwide reached 750 million tons in 2015 (Anjani et al., 2019). The global

* Corresponding author at: Cranfield Water Science Institute, Vincent Building, Cranfield University, Bedfordshire, MK43 0AL, UK

E-mail address: hermassi.mehrez@gmail.com (M. Hermassi)

utilization of fly ash is only 25% of the total production (47% in Europe and 38% in USA) mostly in the construction sector (Anjani et al., 2019).

Moreover, the indiscriminate and long-term use of P fertilizers has become a relevant source of soil and water pollution. Besides the environmental concern of the eutrophication events caused by high P concentration in natural water bodies there is a need to promote its recovery as phosphorous secondary resource. The future supply to the high commercial demand for this element is being compromised due to the scarcity of natural reserves (Álvarez et al., 2018).

The conversion potential of coal fly ash in high quality zeolite-based products have been widely proved and demonstrated in the last decades by applying different synthesis methods such alkaline direct conversion (Holler and Wirsching, 1985), up-scale at pilot plant (Moreno et al., 2001), alkaline fusion (Rayalu et al., 2000, 2001), using Si-extracts and Al-rich liquid wastes (Moreno et al., 2002) and also using gasification fly ash as starting material (Font et al., 2009). The porous structure and high cationic exchange capacity (CEC) of some zeolites (certain Na-zeolites attain up to 5 m-eq/kg), including that of the zeolitic products synthesized from fly ash, give them a high potential to be applied in different fields.

Numerous studies and field applications of these minerals have been reported, providing environmental and technological solutions to the aforementioned industrial activities, including: i) the uptake of pollutants from wastewaters (Itkos et al., 2010; Moreno et al., 2001; Querol et al., 2006; Balsamo et al., 2012, 2010); ii) agriculture (Guaya et al., 2018; Gholamhoseini et al., 2013); iii) ecological restoration and soil amendments (Buondonno et al., 2013; Burger et al., 2011; Larney and Angers, 2012; Vallejo et al., 2012); and iv) organics waste composting (Nissen et al., 2000; Villaseñor et al., 2011; Zorpas et al., 2000). Attention has also been paid to the synthesis of K-zeolites from fly ash and its potential applications have also been of interest and lead to a series of studies focused mainly on the synthesis of phillipsite and chabazite for potential agriculture purposes (Amrhein et al., 1996; Murayama et al., 2008; Querol et al., 1997; Zeng et al., 2002) The interest on K-zeolites has been grown in the last years in view of its potential application in agriculture as slow release fertilizers. The published CEC of K-zeolites synthesized from Fly Ash (FA) ranged from 1.9 to 3.8 m-eq/kg are summarized in Table 1 (Pramatha and Prabir, 2003; Li et al., 2014). The slow release of K from the zeolite compared with that of other fertilizers, allows reducing leaching losses. In addition, the porous structure of zeolites permits the retention of other nutrients (mainly Nitrogen (N)) increasing the uptake by plants. The aforementioned factors increase the absorption of essential nutrients in plants with a consequent increase in crop yields, overall plant growth and are therefore a suitable material for the regeneration and recovery of degraded land, mines, quarries, etc. The application of these zeolites may be beneficial to reduce application rates of chemical fertilizers, thereby improving the sustainability of restoration activities and agricultural systems. The use of loaded K-zeolites with

other essential nutrients such Phosphorous (P), is of a key interest for the aforesaid purposes.

The recovery and recycling of P from wastewater effluents and waste materials provides a key opportunity to reduce the P import dependency from third markets. Recovery and re-use of P within hitherto unexploited solid and aqueous waste streams may further serve to reduce pressure on limited phosphate rock reserves and may also reduce energy and/or material requirements for P acquisition (Wendling et al., 2013). It is well known that the reduction of P discharges into water receiving bodies is needed to prevent eutrophication, and consequently, legislation on P rejects for municipal wastewater treatment plants (WWTPs) is becoming more stringent in Europe (2000/60/EC, Barca et al., 2013). Therefore, research on low-cost techniques to upgrade P removal has become a priority for scientists in the last two decades.

The high specific surface areas and nanoporous structure and CEC of zeolites make them attractive for phosphate sorption and because of the slow-release of cations from the zeolite cages they can be used as slow-release fertilizers for plants (Watanabe et al., 2014). The use of ammonium charged zeolites as a slow-release fertilizer has been reported (Zwingmann et al., 2011) and also that of K-zeolites synthesized from FA with the addition of Ca and ammonium (Li et al., 2014). However, the incorporation of phosphate in addition to ammonium and potassium ions for a NPK fertilizer is a challenge to be achieved taking into account that anions (e.g., HPO_4^{2-}) are rejected from zeolite structures by the Donnan exclusion principle. Previous works demonstrated that modified zeolites synthesized from fly ash (Ca_NaP1) can be an effective sorbent for P from wastewaters (Hermassi et al., 2016b, 2016a).

The aim of this study is to evaluate the feasibility of using coal fly ash (FA-TE and FA-LB) for the synthesis of K-zeolites and subsequent use as a sorbent material for the recovery of phosphate from treated wastewater effluents. Different synthesis conditions (temperature, KOH concentration, KOH-solution/FA ratio and activation time) were applied to optimize the synthesis from both FA and establish differences according to the mineralogy and chemistry of FA to obtain suitable zeolitic products for P uptake from water. Special attention was paid on the synthesis of Ca-bearing K-zeolites such merlinoite and chabazite due to the key role of Ca in the subsequent uptake of P from waters as stated in previous studies (Hermassi et al., 2016b, 2016a). Two different zeolitic products from FA-TE and FA-LB were selected for subsequent study of their phosphate sorption capacity. The P sorption was tested under several experimental conditions on the optimal zeolitic products selected from each FA. The results of the P sorption are presented in terms of equilibrium isotherm and sorption kinetics. The homogeneous particle diffusion (HPDM) and shell progressive (SPM) models were used to describe the kinetic data for the K-zeolitic products.

2. Experimental

2.1. Fly ash samples

Around 20 kg of fly ash samples were supplied from two Spanish coal power plants: Andorra-Teruel 1050 MW (FA-TE) and Los Barrios 550 MW (FA-LB). These coal fly ashes were first characterized and subsequently used as starting material for the synthesis of K-zeolites.

Mineralogical composition of FA-TE and FA-LB samples was determined by X-Ray Powder Diffraction (XRD) using a Bruker D8 Advance diffractometer with monochromatic $\text{Cu K}\alpha 1,2$ radiation ($\lambda = 15,405$) operated at 40 kV and 40 mA. The primary parallel X-ray beam was generated by a Göbbel mirror and the scattered beam was analysed by a Sol-X detector with the following scanning parameters: from 4 at 120° of 2θ , a step size of 0.018° , and time per step of 9 s. The crystalline phase identification was carried out by means the EVA software (from

Table 1
CEC of the synthetic K-zeolite products by FA conversion.

Zeolite form	CEC (eq/kg)
K-H ($\text{K}_2\text{Al}_2\text{Si}_4\text{O}_{12}\cdot\text{H}_2\text{O}$)	3.7–3.8
W or K-M (equivalent to natural phillipsite ($\text{K}_2(\text{Al}_2\text{Si}_3\text{O}_{10}\text{H}_2\text{O}))$)	1.9
Erionite ($(\text{Na}_4\text{Ca}_2\text{K}_4)(\text{Al}_4\text{Si}_{14}\text{O}_{36})15\text{H}_2\text{O}$)	3.1
Chabazite ($\text{CaAl}_2\text{Si}_4\text{O}_{12}\text{H}_2\text{O}$)	3.8
Q-zeolite ($7\text{K}_2\text{O}\cdot 7\text{Al}_2\text{O}_3\cdot 14\text{SiO}_2\cdot 21.7\text{H}_2\text{O}$)	1.9
F-zeolite ($\text{KAlSiO}_4\text{H}_2\text{O}$)	1.9
Merlinoite zeolitic products	3.2

Bruker), which use the ICDD database (<http://www.icdd.com/pdf-2/>). Subsequently, Rietveld method was undertaken for FA-TE and FA-FB diffraction pattern using TOPAS Academic Software (Bruker AXS TOPAS, 2000), which uses a linear least squares method to predict the measured X-ray diffraction pattern. The parameters used in the fitting calculation include the lattice parameters for each phase, the occupancy of each atom in the unit cell, background coefficients, zero-shift error, the scale factor (relative intensity of each phase), and the effects of crystallite size. The goodness of the fit was evaluated using the lower weighted profile R-factor, Rwp (Young, 1995). The determination of amorphous content in fly ash samples was carried out by use of pure CaF₂ as internal standard (XRD patterns for both FA are reported in Supplementary material).

For chemical analysis samples were acid-digested by using a two-step digestion method devised by for coal and coal ashes by Querol et al. (1995). The resulting solution was then analysed by Inductively-Coupled Plasma Atomic-Emission Spectrometry (ICP-AES, IRIS Advantage TJA Solutions, THERMO) and by Inductively-Coupled Plasma Mass Spectrometry (ICP-MS, X Series II, THERMO) for 57 major and trace elements, respectively as summarized in Table 2. The international reference material NBS1633b was also used to determine the accuracy of the analytical and digestion methods.

The European Standard leaching test EN-12457 (according to Council decision 2003/33/EC) was applied to the fly ash samples to determine the leaching potential of major and trace elements. The pH and ionic conductivity of the leachate samples were determined by conventional methods. The content of major, minor and trace elements of the leachates were determined by ICP-AES and ICPMS.

2.2. Synthesis of K-zeolites

The synthesis of K-zeolites was performed on FA-TE and FA-LB by applying the conventional hydrothermal conversion method in a 125 mL PARR 4744 reactor using KOH solutions of 1, 3, and 5 M, KOH-solution/FA ratio of 2 and 4 L/kg, synthesis temperatures of 150 and 200 °C, and 8, 16, and 24 h of conversion time. The K-zeolitic products obtained were first washed to remove the excess of KOH and air dried prior to analysis. The mineralogy of the K-zeolitic products was analysed by the same method previously reported for FA. The cation exchange capacity (CEC) of the K-zeolitic products was measured by applying the ISRIC method. This method applies a NH₄Cl/zeolite closed batch using a ratio of 1 g of zeolite and 100 mL of NH₄Cl to ensure the maximum CEC, at 25 °C and 1 h of stirring. The ammonium of the resulting batch solution was measured by a selective ammonium electrode (Orion 9512H-PBNWP) and the CEC was calculated taking into account the initial concentration of ammonium and that remaining in solution after the batch.

XRD analysis for K-zeolitic products was determined as the same method as the FA described in Section 2.1. The Reference Intensity Ratio (RIR) method was used for crystalline phase quantification of the zeolitic products (de Wolf and Visser, 1988). The RIR method uses always the corundum as the internal standard (RIRcor, Hubbard and Snyder, 1988; Hillier, 2000). RIR values of the more intense peak of each phase respect to the corundum (50,50) are obtained from the PDF-2 database of International Centre for Diffraction Data (ICDD).

2.3. Phosphate-removal equilibrium experiments

Phosphate test solutions were prepared by dissolving a weighed amount of Na₂HPO₄·H₂O in water obtained from a Milli-Q-Academic-A10 apparatus (Millipore Co. France). Batch experiments were performed at room temperature (22 ± 1 °C). Weighted amounts of dry KP1 zeolites samples (0.2 g) were shaken overnight with 12 mL of aqueous solutions containing different initial concentrations of phos-

Table 2
Bulk and leachable concentrations of major and trace elements in the FA-TE and FA-LB.

	Bulk content		pH	Leachates	
	FA-TE	FA-LB		FA-TE	FA-LB
				8,2	8,1
%			mg/kg		
Al ₂ O ₃	25,8	20,2	Al	<0,1	<0,1
CaO	3,8	2,1	Ca	2107	2329
Fe ₂ O ₃	17,4	7,0	Fe	<0,1	<0,1
K ₂ O	1,3	2,3	K	101,1	<0,1
MgO	1,1	2,2	Mg	0,6	<0,1
Na ₂ O	0,2	1,1	Na	41,2	<0,1
P ₂ O ₅			P	<0,1	<0,1
SO ₃	0,6	0,5	SO ₄ ²⁻	5114	<0,1
mg/kg					
Li	273	85	Li	19	2,6
Be	12	4,6	Be	<0,01	<0,01
B	311	346	B	77,9	134,4
Sc	25	23	Sc	<0,01	<0,01
Ti	5557	5811	Ti	<0,01	<0,01
V	215	325	V	0,3	5,3
Cr	129	129	Cr	0,5	3,8
Mn	377	513	Mn	<0,01	<0,01
Co	31	23	Co	<0,01	<0,01
Ni	45	48	Ni	0,01	0,01
Cu	60	79	Cu	<0,01	<0,01
Zn	276	246	Zn	0,02	0,02
Ga	48	33	Ga	0,81	0,30
Ge	6,9	18	Ge	<0,01	0,02
As	115	32	As	<0,01	0,02
Se	3,3	19	Se	0,4	4,7
Rb	99	102	Rb	0,3	0,2
Sr	749	414	Sr	20,0	15,1
Y	55	38	Y	<0,01	<0,01
Zr	210	149	Zr	<0,01	<0,01
Nb	107	80	Nb	<0,01	<0,01
Mo	12	26	Mo	4,7	14,6
Cd	<0,1	2,6	Cd	<0,01	<0,01
Sn	10	3,6	Sn	<0,01	<0,01
Sb	6	10	Sb	0,08	0,2
Cs	19	9,3	Cs	0,0	0,0
Ba	704	1192	Ba	1,9	1,2
La	77	46	La	<0,01	<0,01
Ce	139	83	Ce	<0,01	<0,01
Pr	18	11	Pr	<0,01	<0,01
Nd	53	35	Nd	<0,01	<0,01
Sm	11	7,5	Sm	<0,01	<0,01
Eu	2,1	1,6	Eu	<0,01	<0,01
Gd	10	7,0	Gd	<0,01	<0,01
Tb	1,6	1,0	Tb	<0,01	<0,01
Dy	9,2	6,4	Dy	<0,01	<0,01
Ho	2,0	1,4	Ho	<0,01	<0,01
Er	5,7	4,1	Er	<0,01	<0,01
Tm	0,8	<0,1	Tm	<0,01	<0,01
Yb	4,8	3,6	Yb	<0,01	<0,01
Lu	<0,1	<0,1	Lu	<0,01	<0,01
Hf	5,6	4,1	Hf	<0,01	<0,01
Ta	23	19	Ta	<0,01	<0,01
W	33	14	W	5,2	2,1
Tl	1,6	2,3	Tl	<0,01	<0,01
Pb	58	29	Pb	<0,01	<0,01

Table 2 (Continued)

	Bulk content		pH	Leachates	
	FA-TE	FA-LB		FA-TE	FA-LB
				8,2	8,1
Bi	2,0	<0,1	Bi	<0,01	<0,01
Th	27	14	Th	<0,01	<0,01
U	14	7,8	U	<0,01	<0,01

phate (100–10,000 mgP-PO₄/L). The pH was fixed using 0.1 mol/L HCl or NaOH solution. After phase separation with a 0.2- μ m syringe filter, the equilibrium pH was measured using a pH electrode (Crison GLP22), and the total phosphate concentration was measured using spectrophotometric colourimetry (Kitson and Mellon, 1944). The phosphate equilibrium sorption capacity was determined using Eq. (1).

$$q_e = (C_0 - C_e) \frac{v}{m_s} \quad (1)$$

where C₀ (mgP-PO₄/L) and C_e (mgP-PO₄/L) represent the initial and equilibrium total phosphate concentrations, respectively; v (L) is the aqueous solution volume; and m_s (g) is the mass of zeolite.

2.4. Batch kinetic experiments of phosphate removal

Batch kinetic experiments were performed by addition of 0.2 g of KP1-FA in solutions containing 10 and 100 mgP-PO₄/L of initial phosphate concentration. Tubes were mechanically shaken at 200 rpm at room temperature (21 \pm 1 °C) and samples were withdrawn sequentially at given contact times. All tests were performed in duplicate and the average data are reported. Samples were centrifuged for 10 min and filtered using cellulose nitrate membrane filters of 0.45 μ m for Ion chromatography and 0.22 μ m for ICP. Two stages of filtration were used for high content of suspended solids.

2.5. Physicochemical characterisation of zeolitic products after sorption

At the end of the sorption experiments, the KP1 zeolite samples were washed with water to remove interstitial water and then oven-dried at 60 °C for structural and textural analysis. The mineralogical composition was analysed using the same method than the zeolitic products synthesized in this study and describes in Sections 2.1 and 2.2.

The point of zero charge (PZC) values of KP1-TE and KP1-LB were determined, and the common intersection point (CIP) method was applied to the titration curves obtained at different ionic strengths. First, an amount of KP1 zeolite (0.1 g) was equilibrated in of deionized water (25 mL) and 0.01 and 0.05 M NaCl solutions (pH from 3 to 11) for 24 h at 200 rpm and 21 \pm 1 °C. The final pH was measured in a Crison GLP21 potentiometer, and the PZC was determined as the pH at which the addition of the sample did not induce a shift in the pH (Δ pH = pH_f - pH_i = 0). All measurements were performed in triplicate, and the average values are reported.

2.6. Phosphate sorption equilibrium modelling

The Langmuir (Eq. (2)) and Freundlich isotherms (Eq. (3)) were used to describe the phosphate sorption:

$$q = \frac{K_L q_m C_e}{1 + K_L C_e} \quad (2)$$

$$\log q_e = \log K_f + \frac{1}{n} \log C_e \quad (3)$$

where C_e (mgP-PO₄/L) and q_e (mgP-PO₄/g) are the equilibrium total phosphate concentrations in the aqueous and solid phases, respectively; q_m (mgP-PO₄/g) is the maximum sorption capacity; K_L (L/mgP-PO₄) is the Langmuir sorption equilibrium constant; n is a constant indicating the Freundlich isotherm curvature; and K_f ((mgP-PO₄/g)/(mg/L)ⁿ) is the Freundlich equilibrium constant.

2.7. Phosphate sorption kinetic modelling

The homogeneous particle diffusion (HPDM) and shell progressive (SPM) models (Liberti and Passino, 1977; Valderrama et al., 2010) were used to describe the kinetic data. Both models assume that the extraction mechanism involves the diffusion of phosphate ions (H₂PO₄⁻ and HPO₄²⁻) from solution into the zeolite (KP1-FA) phase through a number of possible pathways: diffusion across the liquid film surrounding the KP1-FA particle; transfer across the solution/particle interface; diffusion into the bulk of the KP1-FA particle; and possible interactions with reactive groups on the FA surface.

Homogeneous Particle Diffusion Model (HPDM):

Describes the diffusion of phosphate ions on the KZ particle as a quasi-homogeneous media

$$i) \text{ for particle diffusion rate control : } -\ln(1 - X^2(t)) = 2 \frac{\pi^2 D_e}{r^2} t \quad (4)$$

$$ii) \text{ for liquid film diffusion control : } -\ln(1 - X(t)) = \frac{3D_e C_{A0}}{r C_r} t \quad (5)$$

Shell progressive model (SPM):

Describes the sorption process in terms of a concentration profile of the solution containing phosphate ions advancing into a partially sorbed saturated spherical KP1-FA particle ("Shell Progressive"):

$$a) \text{ for fluid film : } X(t) = \frac{3C_{A0} K_F}{a_s C_{so}} t \quad (6)$$

$$b) \text{ for particle diffusion : } \left[3 - 3(1 - X(t))^{\frac{2}{3}} - 2X(t) \right] = \frac{6D_e C_{A0}}{a_s^2 C_{so}} t \quad (7)$$

$$c) \text{ for chemical reaction : } \left[1 - (1 - X(t))^{1/3} \right] = \frac{K_s C_{A0}}{r} t \quad (8)$$

where X(t) is the fractional attainment of equilibrium at time t, C is the total concentration of sorbing species; C_r is the total concentration of sorbing in the KP1-FA phase; D_e the effective diffusion coefficient of ammonium ions in the zeolite phase (m²s⁻¹), r the radius of the zeolite particle assumed to be spherical (m). X(t) values could be calculated by using Eq. (9):

$$X(t) = \frac{q_t}{q_e} \quad (9)$$

where q_t and q_e are phosphate loading on the particle phase at time t and when equilibrium is attained (mg-g⁻¹) respectively. All experimental data were treated graphically and compared to all fractional attainment of equilibrium functions (F(X) = f(t)) (Eqs. (4)–(9)).

3. Results and discussion

3.1. Characterisation of fly ash samples

FA-TE and FA-LB are primarily composed of Al-Si glass (77 and 74%, respectively) with different proportions of crystalline phases. FA-TE shows relatively high proportions (14%) of mullite (Al₆Si₂O₁₃), low proportion (6%) of quartz (SiO₂), and of Fe-oxides (1.5% maghemite,

Fe₂O₃, and 1.2% hematite, Fe₂O₃), and traces of anhydrite (CaSO₄) and calcite (CaCO₃). Quartz (18%) is the main crystalline phase present in FA-LB and also contains minor amounts of mullite (7%) and traces of hematite and calcite (<0.5%). The R_{wp} obtained in FA-TE and FA-LB measurements were 4.68 and 7.55, respectively, which indicate an accurate Rietveld refinement. The chemical composition of FA-TE is dominated by relatively high concentrations of Al₂O₃ (26%), Fe₂O₃ (17%), CaO (3.8%), and SO₃ (0.6%) when compared with LB-FA (Table 2). The relatively high Fe, S, and Ca content in the TE-FA, and related crystalline phases (Fe-oxides, anhydrite and calcite) is due to the predominant use of a local subbituminous coal rich in pyrite in the feed coal blend. Fe-oxides, anhydrite and calcite are non-reactive phases in alkaline hydroxides solutions. Consequently, the Ca present (calcite and anhydrite) is not available for the synthesis of Ca-bearing K-zeolites. Hematite and magnetite crystallize on the fly ash surface then limiting the dissolution of glass components (Al, Si, Ca) reducing the available amount of these elements for synthesis of zeolites.

The occurrence of calcite in both FA-TE and FA-LB give rise to the slightly alkaline pH of the leachates from FA-TE (8.2) and FA-LB (8.1) (Table 2). Two relatively high concentrations of S and Ca in the FA-TE

leachates and Ca in FA-LB leachates are in agreement with the occurrence of anhydrite and calcite in FA (Table 2). Regarding the leaching potential of trace elements only the leachable concentrations of Se (4.7 mg/kg) and Mo (41.6 mg/kg) from FA-LB are of special concern as exceed the limit values for non-hazardous materials established by the EC 33/2003 decision for the disposal of solid residues in landfilling (Table 2).

3.2. Synthesis of K-zeolites from fly ash

The synthesis of K-zeolites from FA-TE and FA-LB by KOH hydrothermal direct conversion give rise to zeolitic products composed by variable proportions of a single zeolite, such W, merlinoite, perliolite (or L), K-H, and megakalsilite or by mixtures of the aforementioned zeolites and/or with natrolite, erionite, chabazite, tobermorite, and ZSM5 and chabazite/natrolite mixtures (Tables 2–3 and Figs. 1–2). The conversion of FA to zeolitic products is consistent with the strength of synthesis conditions applied, generally increasing as the synthesis temperature, KOH-solution/FA ratio, KOH concentration and activation

Table 3

Proportion (%) of relict phases (according to the re-calculated content in FA-TE), (26% Qz and 61% Mu) and synthesized zeolites in the zeolitic products obtained by KOH hydrothermal conversion at different synthesis conditions from TE-FA and CEC values. Qz: quartz; Mull: mullite; Mer: merlinoite; Cha: chabazite; Kal: megakalsilite; Tb: tobermorite; Eri: erionite. nd: not determined. T: temperature; L/S: KOH-solution/FA ratio; KOH: solution concentration; t: activation time.

Synthesis conditions	Relict phases			Zeolite											Relict phases			CEC	
	Qz	Mu	W	Mer	Nat	Cha	K-H	L	F	Kal	Tob	Eri	Total	Total					
150 °C	2 L/ Kg	1 M	8 h	31	45	0	0	0	0	0	0	0	0	0	0	0	100	0	nd
			16 h	25	44	0	0	0	0	0	0	0	0	0	0	0	100	0	nd
		3 M	8 h	20	33	20	0	0	0	0	0	0	0	0	0	0	79	20	3,8
			16 h	23	33	20	0	0	0	0	0	0	0	0	0	0	100	0	nd
		5 M	8 h	14	25	39	0	0	0	0	0	0	0	0	0	0	61	39	3,3
			16 h	19	27	27	0	0	11	0	0	0	0	0	0	0	62	38	nd
	4 L/kg	1 M	8 h	12	34	0	0	13	16	0	0	0	0	0	0	0	71	29	3,8
			16 h	4	19	0	0	11	23	0	0	0	0	0	0	0	36	64	nd
		3 M	8 h	0	9	23	0	30	0	20	0	0	0	0	0	0	27	73	nd
			16 h	28	39	0	0	0	0	0	0	0	0	0	0	0	100	0	nd
		5 M	8 h	21	48	0	0	0	0	0	0	0	0	0	0	0	100	0	nd
			16 h	18	43	0	0	0	0	0	0	0	0	0	0	0	100	0	nd
	200 °C	2 L/kg	1 M	8 h	21	48	0	0	0	0	0	0	0	0	0	0	100	0	nd
				16 h	18	46	0	0	0	0	0	0	0	0	0	0	100	0	nd
			3 M	8 h	8	20	50	0	0	0	0	0	0	0	0	0	50	50	2,3
				16 h	7	20	0	0	0	0	0	0	33	19	0	0	47	52	2,8
			5 M	8 h	0	20	0	0	0	0	0	0	37	27	0	0	36	64	2,8
				16 h	0	8	57	0	0	0	0	27	0	0	0	0	16	84	3,2
4 L/kg		1 M	8 h	16	38	0	0	0	0	18	0	0	0	0	0	82	18	nd	
			16 h	17	31	30	0	0	0	0	0	0	0	0	0	70	30	nd	
		3 M	8 h	14	31	29	0	0	0	0	0	0	0	0	0	71	29	nd	
			16 h	6	37	0	0	0	0	32	0	0	0	0	0	68	32	nd	
		5 M	8 h	6	21	53	0	0	0	0	0	0	0	0	0	47	53	2,6	
			16 h	5	18	33	24	0	0	0	0	0	0	0	0	42	57	3,4	
4 L/kg		1 M	8 h	0	5	0	0	30	0	0	1	0	41	0	0	25	72	nd	
			16 h	0	0	0	0	8	0	0	1	0	65	0	10	15	84	1,9	
		3 M	8 h	0	0	0	0	0	0	0	12	0	72	5	0	10	89	nd	
			16 h	0	0	0	0	0	0	40	0	0	0	0	0	60	40	2,2	
		5 M	8 h	10	36	0	54	0	0	0	0	0	0	0	0	46	54	nd	
			16 h	12	23	0	65	0	0	0	0	0	0	0	0	35	65	4,5	
4 L/kg	1 M	8 h	0	32	0	0	0	0	58	0	0	0	0	0	42	58	3,1		
		16 h	0	4	0	0	0	0	0	0	0	0	0	0	4	96	2,9		
	3 M	8 h	0	0	0	0	0	0	50	50	0	0	0	0	0	100	nd		
		16 h	0	0	0	0	0	0	0	0	100	0	0	0	0	100	nd		
	5 M	8 h	0	0	0	0	0	0	0	0	100	0	0	0	0	100	nd		
		16 h	0	0	0	0	0	0	0	0	100	0	0	0	0	100	nd		
24 h	0	0	0	0	0	0	0	0	0	100	0	0	0	0	100	2,5			

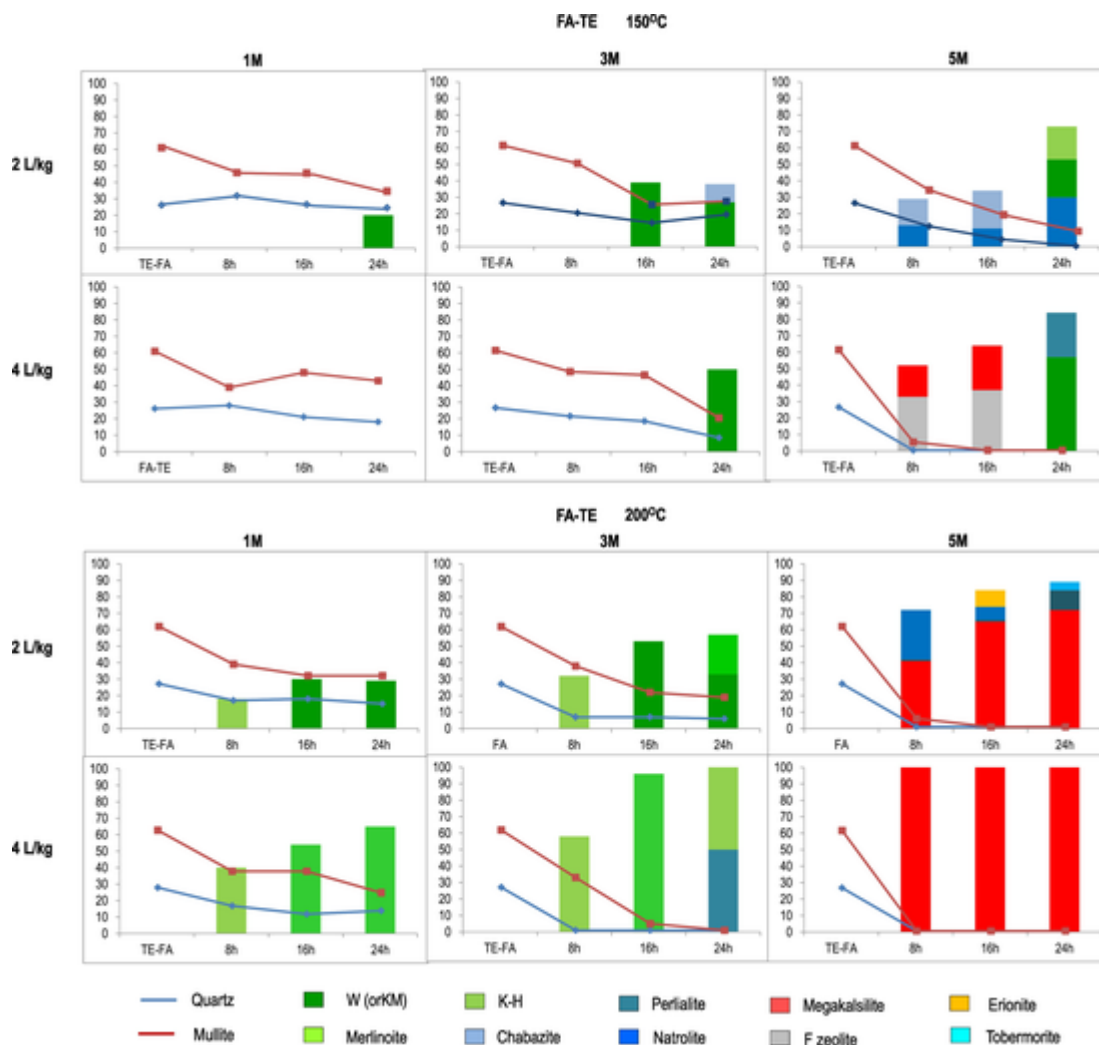


Fig. 1. Proportion of relict quartz and mullite and that of the synthesized zeolites from FA-TE according to the synthesis temperature, KOH-solution/FA ratio, KOH concentration and activation time.

time increases. The proportion of zeolites synthesized from FA is then also consistent with the dissolution of Si and Al from glass, quartz, and mullite according to Querol et al. (1997) the dissolution of the mentioned phases from FA are glass > quartz > mullite and its subsequent precipitation in the zeolite structure (Tables 2–3 and Figs. 1–2).

W Zeolite (20–57% of the crystalline phases in the zeolitic products), merlinoite (24–96%), K-H zeolite (18–58%), and low CEC megakalsilite (19–100%) are the primarily zeolites produced in most of the zeolitic products from FA-TE (Table 3 and Fig. 1). Natrolite (8–30%), Perialite (1–50%), F zeolite (33–37%), chabazite (16–23%), erionite (10%), and tobermorite (5%) are also synthesized in specific synthesis conditions (Table 3 and Fig. 1).

The conversion to zeolites from FA-TE is relatively poor (0–39%) at low temperature (150 °C) and low KOH-solution/FA ratio (2 L/kg) for most of the KOH concentrations and activation time applied. At the synthesis temperature (150 °C) and KOH-solution/FA ratio (2 L/kg) low amounts of W zeolite (20–39%) are synthesized for low (1 M) and intermediate (3 M) KOH concentrations and after long activation time (24 h for KOH 1 M and 16–24 for KOH 3 M). The extremely low proportion of quartz dissolved (with respect to its initial content in FA), even lower than that of mullite (Table 3 and Fig. 1) accounts for the low conversion efficiency and for the synthesis of low proportions of zeolite W, a zeolite with low Si/Al ratio (<2). Mixtures of chabazite and natrolite (16–13% and 23–11%), are produced when increasing

KOH concentration to 5 M for activation times of 8–16 h, keeping the temperature at 150 °C and KOH-solution/FA ratio at 2 L/kg. The synthesis of chabazite, with a slightly higher Si/Al ratio (2) than W, matches with a slightly higher dissolution of quartz vs mullite (Table 3 and Fig. 1). The results from this study and those from other authors (Amrhein et al., 1996; Murayama et al., 2002a, 2002b; Querol et al., 1997) indicates that low synthesis temperatures (100–150 °C) are required to obtain chabazite. Even the low proportions obtained, the synthesis of Ca-bearing chabazite using relatively low temperature (150 °C), low KOH-solution/FA ratio (2 L/kg), and low activation times (8–16 h) reported in this study is of interest for its potential use as phosphate sorbent material.

Increasing the KOH-solution/FA ratio to 4 L/kg and keeping temperature at 150 °C the conversion of FA-TE to zeolite, is even lower than at 2 L/kg when applying KOH concentration of 1–3 M (Table 3 and Fig. 1). At the mentioned synthesis conditions, the only zeolitic product is a 50% W zeolitic material, which is obtained for KOH concentration of 3 M and 24 h activation time (Table 3 and Fig. 1). Increasing the KOH concentration to 5 M the dissolution of quartz and mullite reached high proportions (73–100% and 67–87%, respectively) (Table 2 and Fig. 2) giving rise to mixtures of low Si/Al ratio zeolites such as F (Al/Si ratio = 1.5) and megakalsilite (1,1) for activation times of 8–16 h and to a rich zeolitic product (84% zeolite) containing a mixture of W (57%) and perialite (27%) (Table 2 and Fig. 2).

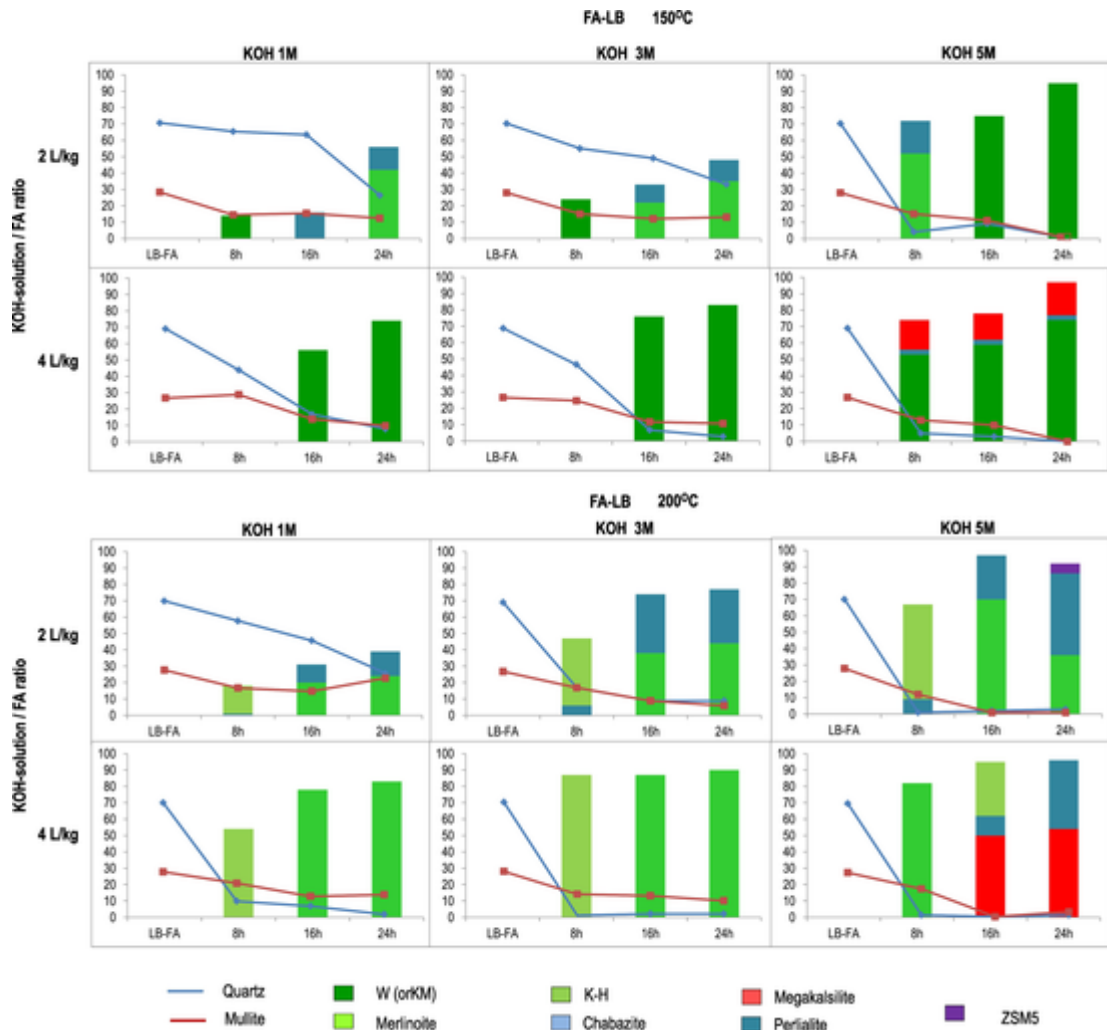


Fig. 2. Proportion of relict quartz and mullite and that of the synthesized zeolites from FA-LB according to the synthesis temperature, KOH-solution/FA ratio, KOH concentration and activation time.

The increase of the synthesis temperature to 200 °C results in higher conversion of FA-TE (40–100%) (Table 2 and Fig. 2), particularly at low KOH-solution/FA ratio (2 L/kg), low KOH concentration (1–3 M) and short activation time (8–16 h), than obtained at low temperature (150 °C) and KOH-solution/FA ratio of 2–4 L/kg, KOH concentrations of 1–3 M and from 8 to 24 h activation time. At this high temperature (200 °C) the following zeolitic products are synthesized: i) single K-H (18–58%, mainly at KOH concentration 1–3 M and after 8 h activation time either at KOH solution/FA ratio of 2 and 4 L/kg); ii) single W zeolitic products (29–53%, mainly at low KOH solution/FA ratio (2 L/kg), KOH concentration of 1–3 M and activation times from 16 to 24 h); iii) Merlinoite-rich products (54–96%, primarily at high KOH-solution/FA ratio (4 L/kg), from 1 to 3 M of KOH concentration and activation times from 16 to 24 h); and iv) A 50:50 mixture of K-H and perialite is synthesized at KOH-solution/FA ratio of 4 L/kg, KOH concentration of 3-M and 24 h activation time. The increase of the KOH concentration to 5 M give rise to the complete dissolution of quartz and mullite and the synthesis of 100% megakalsilite products at high KOH-solution/FA ratios (4 L/kg) and megakalsilite rich products (41–72%) when reducing the KOH-solution/FA ratio to 2 L/kg. The megakalsilite rich products also contains 8–30% of natrolite (at activation times of 16 and 8 h, respectively) and low proportions of high Si/Al zeolite (>10) such erionite (10%, at 16 h activation time) and tobermorite (5%, at 24 h activation time).

Regarding the synthesis of K-zeolite from FA-LB, the conversion to zeolite is reached easily and yield higher values than for FA-TE (Tables 2–3 and Figs. 1–2). This conversion is due to the low Fe-bearing phases present on the LB-FA surface that favors the dissolution of the reactive phases from FA. At the weakest synthesis conditions (temperature of 150 °C, KOH-solution/FA ratio of 2 L/kg, KOH concentration of 1 M and 8 h activation time) a zeolitic product containing 14% of single W zeolite is already synthesized. Increasing the KOH concentration from 1 to 5 M and the activation time from 8 to 24 h, both the higher occurrence and easy dissolution of quartz with respect mullite results first in the synthesis of relatively high Si/Al ratio zeolites such merlinoite (Si/Al = 2.4) and perialite (Si/Al = 3) (Table 4 and Fig. 2). The almost complete dissolution of quartz and mullite when applying high KOH concentration (5 M) and long activation times (16–24 h) results in the synthesis of relatively high proportions of W zeolite (75–95%) indicating that a higher proportion of Al is available to reduce the Si/Al ratio in the dissolved solution from FA and form zeolites with a slightly lower Si/Al ratio than merlinoite. The use of high KOH-solution/FA ratios (4 L/kg) favors the simultaneous dissolution of high proportions of quartz and mullite enhancing the synthesis of W (53–83%) instead merlinoite. At high KOH-solution/FA ratios (4 L/kg) and high KOH concentrations (5 M) besides high proportions of W zeolite (53–74%) significant proportions of megakalsilite (16–20%) are also synthesized.

Table 4
Proportion (%) of reactive relict phases (according to the re-calculated content in FA-TE), (69% Qz and 27% Mu) and zeolites in the zeolitic products obtained by KOH hydrothermal conversion at different synthesis conditions from LB-FA and CEC values. Qz: quartz, Mull: mullite; Mer: merlinoite; Cha: Chabazite; Kal: megakalsilite; Tb: tobermorite; Eri: erionite. nd: not determined. T: temperature; L/S: KOH-solution/FA ratio; KOH: solution concentration; t: activation time.

Synthesis conditions				Reactive relict phases											Zeolite		Relict phases	Zeolite	CEC		
T	L/S	KOH	t	Qz	Mull	W	Mer	Nat	Cha	K-H					Tob	Eri	Total	Total	CEC		
150 °C	2 L/kg	1 M	8 h	64	13	14	0	0	0	0	0	0	0	0	0	0	86	14	nd		
			16 h	62	14	0	0	0	0	0	0	16	0	0	0	0	83	16	1.5		
			24 h	25	11	0	42	0	0	0	0	14	0	0	0	0	44	56	nd		
		3 M	8 h	54	14	24	0	0	0	0	0	0	0	0	0	0	76	24	2.8		
			16 h	48	11	0	22	0	0	0	0	11	0	0	0	0	66	33	nd		
			24 h	32	12	0	35	0	0	0	0	13	0	0	0	0	51	48	nd		
	5 M	8 h	3	14	0	52	0	0	0	0	20	0	0	0	0	27	72	nd			
		16 h	8	10	75	0	0	0	0	0	0	0	0	0	0	25	75	nd			
		24 h	0	0	95	0	0	0	0	0	0	0	0	0	0	5	95	nd			
	4 L/kg	1 M	8 h	8 h	44	29	0	0	0	0	0	0	0	0	0	0	100	0	nd		
				16 h	17	14	56	0	0	0	0	0	0	0	0	0	44	56	3.1		
				24 h	1	13	0	83	0	0	0	0	0	0	0	0	26	74	2.6		
			3 M	8 h	47	25	0	0	0	0	0	0	0	0	0	0	100	0	nd		
				16 h	7	12	76	0	0	0	0	0	0	0	0	0	24	76	2.5		
				24 h	3	11	83	0	0	0	0	0	0	0	0	0	17	83	2.0		
		5 M	8 h	5	13	53	0	0	0	0	0	3	0	18	0	0	26	0	2.3		
			16 h	3	10	59	0	0	0	0	0	3	0	16	0	0	21	76	2.0		
			24 h	0	0	74	0	0	0	0	0	3	0	20	0	0	3	83	1.7		
		200 °C	2 L/kg	1 M	8 h	57	16	0	0	0	0	17	1	0	0	0	0	82	18	nd	
					16 h	45	14	0	20	0	0	0	11	0	0	0	0	69	31	2.6	
					24 h	25	22	0	24	0	0	0	15	0	0	0	0	61	39	nd	
				3 M	8 h	17	17	0	0	0	0	0	41	6	0	0	0	0	53	47	2.1
					16 h	9	9	0	38	0	0	0	36	0	0	0	0	0	26	74	3.3
					24 h	9	6	0	44	0	0	0	33	0	0	0	0	0	24	77	2.1
5 M			8 h	0	11	0	0	0	0	0	58	9	0	0	0	0	33	67	2.7		
			16 h	1	0	0	70	8	0	0	27	0	0	0	0	0	3	97	nd		
			24 h	2	0	0	36	0	0	0	50	0	0	0	0	0	8	92	3.8		
4 L/kg	1 M		8 h	8 h	9	20	0	0	0	0	54	0	0	0	0	0	46	54	4.2		
				16 h	6	12	0	78	0	0	0	0	0	0	0	0	22	78	4.7		
				24 h	1	13	0	83	0	0	0	0	0	0	0	0	17	83	3.1		
			3 M	8 h	0	0	0	0	0	0	87	0	0	0	0	0	13	87	nd		
				16 h	1	12	0	87	0	0	0	0	0	0	0	0	13	87	4.6		
				24 h	1	9	0	90	0	0	0	0	0	0	0	0	10	90	3.4		
	5 M		8 h	1	17	0	82	0	0	0	0	0	0	0	0	18	82	2.8			
			16 h	0	0	0	0	0	0	0	33	12	0	50	0	0	0	95	0.8		
			24 h	1	3	0	0	0	0	0	0	42	0	54	0	0	4	96	3.7		

The increase of the synthesis temperature up to 200 °C results in a higher FA conversion to zeolite than at 150 °C for FA-LB (Table 4 and Fig. 2). With the exception of the zeolitic products synthesized at low KOH-solution/FA ratio (2 L/kg) and low KOH concentration (1 M), attaining only 18–39% of the crystalline phases, the zeolites obtained at the remaining synthesis conditions attain high proportions of the zeolitic product (54–97% of the crystalline phases). As stated for FA-TE at this synthesis temperature (200 °C), K-H (17–87%) is generally synthesized when applying low activation times (8 h) either at KOH-solution/FA ratios of 2 and 4 L/kg and KOH concentration from 1 to 5 M. Mixtures of merlinoite (20–74%) and perialite (11–50%) are synthesized at low KOH-solution/FA ratios (2 L/kg) and long activation time (8–24 h), whereas single and rich merlinoite zeolitic products (78–90%) are synthesized at high KOH-solution/FA ratios (4 L/kg), long activation times (16–24 h) but low-intermediate KOH concentrations (1–3 M) or combining high KOH concentration (5 M) and short activation time (8 h). Rich megakalsilite products (50–54%) containing perialite (12–42%) and K-H zeolite (33%) are synthesized when apply-

ing high KOH-solution/FA ratio (4 L/kg), high KOH concentration (5 M) and long activation time (16–24 h).

3.3. K-zeolites: physico-chemical properties

From the comparison of results of the synthesis stage of zeolitic products it can be highlight that:

- Despite for both FA-TE and FA-LB, some zeolitic products are produced at the lowest temperature (150 °C), KOH-solution/FA ratio (2 L/kg), and KOH concentration (1 M), a longer activation time (24 h) is required to achieve the conversion of FA to zeolite for FA-TE than for FA-LB (8 h). Accordingly, the obtained zeolitic products are more easily achieved, in time basis, for FA-LB than for FA-TE due to the low content of non-reactive Fe-bearing phases on the surface of FA.
- Merlinoite and W-zeolite are by far the dominating zeolites in most of the zeolitic products synthesized from FA-LB whereas the zeolitic

products synthesized from FA-TE display a higher variety of zeolites for a given synthesis conditions.

- c) Furthermore Ca-bearing zeolite merlinoite is synthesized at weaker synthesis conditions for FA-LB than for FA-TE, requiring high synthesis temperature (200 °C) for the later. This is due to the high proportion of quartz respect mullite and the high Ca from glass available in FA-LB.
- d) The synthesis of other Ca-bearing zeolites such chabazite is obtained only for FA-TE, applying low temperatures (150 °C), high KOH-concentrations (5 M), low KO-solution/FA ratios (2 L/kg). The high proportion of mullite respect to quartz is most probably the primarily cause for the synthesis of this zeolite (KP1-TE) only in this FA at the synthesis conditions applied.
- e) On the opposite low CEC megakalsilite is readily synthesized and in remarkable proportions from FA-TE than from FA-LB, due to the high content of mullite with respect to quartz that favors the formation of this low Si/Al ratio (1,1) specially when high K supply (KOH-solution/FA ratio) (4 L/kg), high temperature (200 °C) and high KOH concentration (5 M) are applied.

Low cation exchange capacity value for untreated fly ash was $< 100 \text{ mmol}_c/\text{kg}$ (Amrhein et al., 1996), and for most common types of zeolitic tuffs; clinoptilolite values ranging between 1.2 and 2 meq/g; mordenite values $\geq 1 \text{ meq/g}$; phillipsite and chabazite 1.8–2.5 meq/g (Cejka, 2005). However, treating fly ash giving higher CEC values; The CEC for zeolitic product formed from FA-TE giving an average ranges from 1.9 to 3.8 meq/g (Table 3). The highest CEC from FA-TE reached for a natrolite/chabazite rich zeolitic product synthesized at 150 °C, KOH-solution/FA solution of 2 L/kg, KOH concentration of 5 M and 8 h activation time. The CEC of the zeolitic products obtained from FA-LB ranges from 0.8 to 5.3 meq/kg (Table 4). The synthesis of K-H zeolite give rise to the highest CEC values of the FA-LB zeolitic products increasing from 2.1 to 5.3 meq/kg as increase the K-H proportion from 41 to 87%. The highest CEC zeolitic product (5.3 meq/g) is achieved for a K-H rich product (87% of the crystalline phases, Table 4) synthesized from FA at high temperature (200 °C), high KOH-solution/fly ash ratio (4 L/kg), a KOH concentration of 3 M, and after 8 h activation time. The CEC of the zeolitic products containing only merlinoite or W zeolite, or containing also perialite or megakalsilite, range from 1.7 to 4.6 meq/kg. Although it is out of the scope of this work, the aforesaid CEC values indicate a large potential for the uptake of NH_4^+ of the zeolitic products obtained.

For the subsequent P sorption experiments the following zeolitic products (Fig. 3) were selected

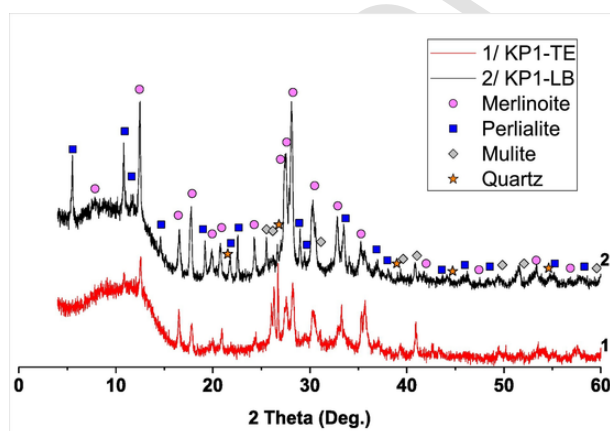


Fig. 3. XRD patterns (merlinoite/W zeolite, perialite, mullite and quartz) of the zeolitic products KP1-TE and KP1-LB selected for the subsequent P sorption experiments.

- a) KP1-TE: a W zeolitic product (30%) synthesized from FA-TE at 150 °C, KOH-solution/FA ratio of 2 L/kg, KOH concentration of 1 M and 24 h.
- b) KP1-LB: a high Merlinoite (52%) and perialite (20%) synthesized from FA-LB at 150 °C, KOH-solution/FA ratio of 2 L/kg, 5 M and 24 h.

The KP1-TE and KP1-LB zeolitics products were selected according to the following issues: a) W and Merlinoite are by far the primarily zeolites produced from FA-TE and FA-LB; b) To compare the P sorption capacity from a K zeolite (W) with a Ca-bearing K zeolite (merlinoite) and c) The synthesis of the aforementioned zeolitic products using weak synthesis conditions (mainly low temperature and low KOH-solution/FA ratio).

The presence of potassium modifies the FA and a pH_{PZC} of 9.3 ± 0.3 was determined for KP1-FA (Fig. 4). Indeed Chen et al. (2006) and Zhang et al. (2007) identified that iron and aluminium surface groups have anions sorption capacity at pH values below the pH_{PZC} . The acid-base characterisation reveals pH_{PZC} values of 4.9 ± 0.5 for FA-TE and 5.1 ± 0.5 for FA-LB (Hermassi et al., 2017b). The higher pH_{PZC} value of KP1 suggests a decrease in the acidity of the metal-hydroxide groups ($\cong \text{MOH}$) of the fly ash structure after modification with potassium salts.

3.4. Phosphate-sorption capacities of KP1-TE and KP1-LB: equilibrium and kinetic performance

3.4.1. Sorption kinetic

Kinetic experiments (q_t versus t) for both zeolites show a different performance as the times to reach equilibrium attainment ($> 90\%$) where 3000 s for KP1-TE and > 8000 s are needed for KP1-LB (Fig. 5).

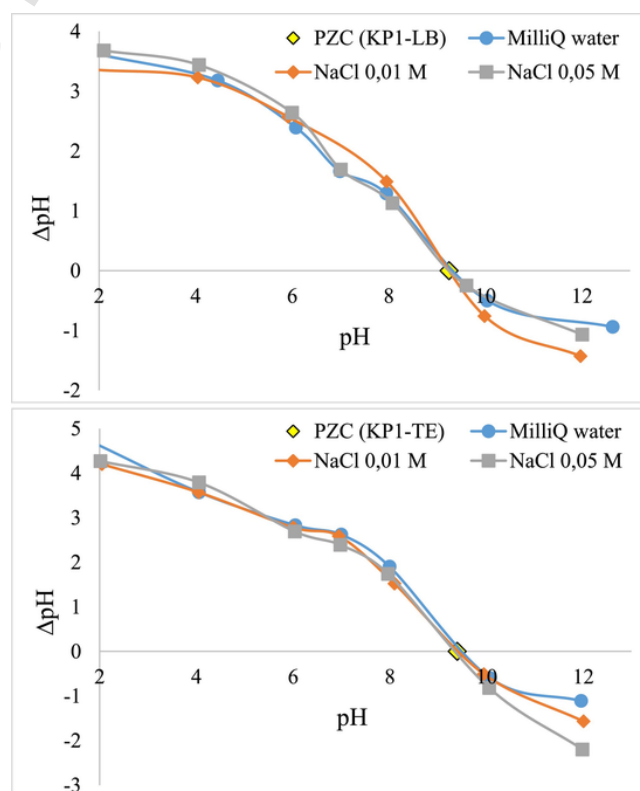


Fig. 4. The variation of ΔpH as a function of the equilibrium pH for the zeolitic products KP1-LB and KP1-TE.

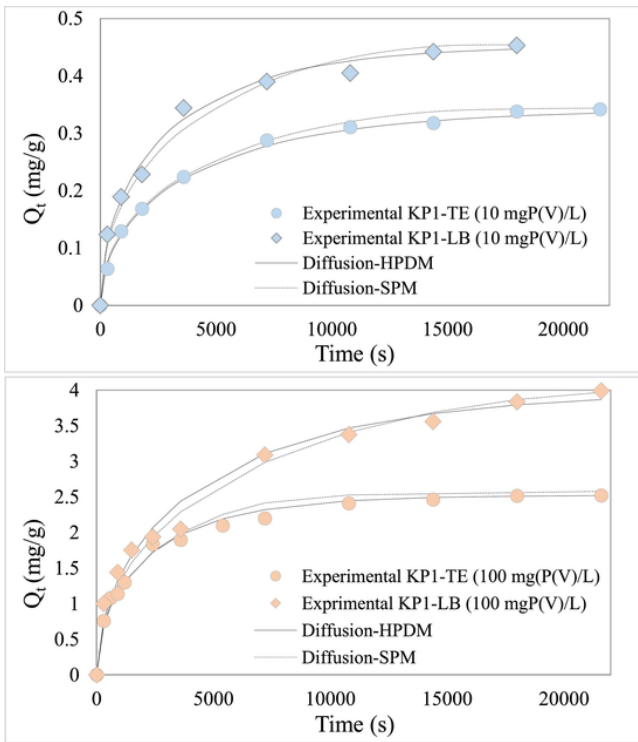


Fig. 5. Kinetic data and predicted curves obtained by linear regression analysis of both models (HPDM and SPM) for KP1-TE and KP1-LB with initial phosphate concentration 10 and 100 mg/L and pH = 8.

Both values for equilibrium attainment are an indication that the phosphate extraction process is based on chemical reactions, as mineral formations, more than a standard anion-exchange process. Values are compatible for stirred reactors needed when working with powder materials as it is the case. Kinetic data were fitted by using the HPDM (Eqs. (4)–(5)) and SPM (Eqs. (6)–(8)) models, results are summarized in Table 5. Both models fit the data satisfactorily for the entire time range of KP1-phase diffusion. The slope values can be used to calculate effective diffusion coefficients for phosphate anions depending on the initial phosphate concentration (10 and 100 mgP-PO₄/L) an average diffusion coefficient for the predominant species is obtained. These calculated diffusion coefficients are in fact a measure of the mean diffusion coefficients of the different species involved in the ion exchange process. The intraparticle mass transfer coefficient can be determined by the effective intraparticle diffusion coefficient D_e . According to the values reported in Table 5, the D_e values are in the range of 10^{-14} – 10^{-13} m²/s and show dependence on the initial phosphate concentration. Such values are common with chemisorption's systems (Walker and Weatherley, 1999). Kinetic parameters were critical in the integration of the synthesized zeolites in stirred reactor based appli-

cations. According to the kinetic parameters, if lower hydraulic residence times is the critical factor the use of KP1TE is recommended- If the selected criteria is increasing the phosphate removal capacity the use of PK1-LB is recommended, however, the hydraulic residence time should be increased.

3.4.2. Sorption equilibrium

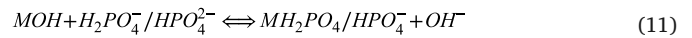
The evaluation of the effects of the initial concentration on phosphate-sorption capacity for both synthesized K-zeolites (KP1-LB and KP1-TE) at fixed pH 8.0 ± 0.2 revealed an important increase as the initial phosphate concentration increased (Fig. 6). Additionally, the equilibrium pH exceeds the initial pH = 8, reaching values as high as 9.4 for KP1-LB and 9.0 for KP1-TE, at lower initial phosphate concentrations (up to 5 mmol P-PO₄/L) and then decreases back to the approximately the initial value for both zeolites. Moreover, the shape of the phosphate-sorption isotherm indicates that KP1-LB has higher affinity for phosphate than KP1-TE, as shown by the higher slope of the (q_e-C_e) function (Fig. 6). The maximum sorption capacities of zeolites were 230 ± 10 mgP-PO₄/g and 130 ± 5 mgP-PO₄/g for KP1-LB and KP1-TE, respectively (Fig. 6).

It should be mentioned that the initial specific surface area (S_{BET}) were carried out using standard methodology described elsewhere (Hermassi et al., 2015), the S_{BET} values for KP1-TE and KP1-LB, were 22.5 and 31.6 m²/g, respectively. Thus, the higher Ca and P contents and larger surface area enhance the phosphate sorption. According to the content of CaO in the zeolitic products and the pH_Z values it is postulated that, the sorption of phosphate ions, mainly H₂PO₄⁻ and HPO₄²⁻, which occurs in the expected pH range (7 to 9) follow the following mechanisms reactions:

- a) Complexation with $\approx MOH_2^+$ surface groups.



- b) Complexation with $\approx MOH$ surface groups.



- c) Formation of calcium phosphate minerals with the Ca(II) in the zeolite structure (CaO):

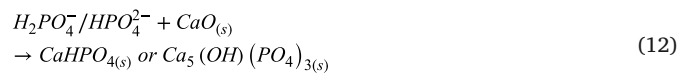


Table 5

Linear regression of HPDM and SPM models for phosphate sorption onto KP1 samples for two different initial phosphate concentration of at initial pH 8 ± 0.2 .

	HPDM			SPM							
	$-\ln(1-X^2)$			$-\ln(1-X)$	X	$[3-3(1-X)^{2/3}-2X]$	$[1-(1-X)^{1/3}]$				
	P(V) ₀ (mg/L)	R ²	D _e	R ²	D	R ²	K _F	R ²	D _e	R ²	k _s
KP1-TE	10	0.98	7.6×10^{-14}	0.95	5.9×10^{-9}	0.80	1.2×10^{-9}	0.99	1.0×10^{-13}	0.96	3.8×10^{-10}
	100	0.99	1.3×10^{-13}	0.95	7.8×10^{-9}	0.81	9.6×10^{-10}	0.99	1.7×10^{-13}	0.96	4.1×10^{-11}
KP1-LB	10	0.99	1.1×10^{-13}	0.95	7.2×10^{-9}	0.79	1.2×10^{-9}	0.99	1.1×10^{-13}	0.95	4.5×10^{-10}
	100	0.99	6.6×10^{-14}	0.96	5.2×10^{-9}	0.88	1.1×10^{-9}	0.99	7.2×10^{-14}	0.95	3.5×10^{-11}

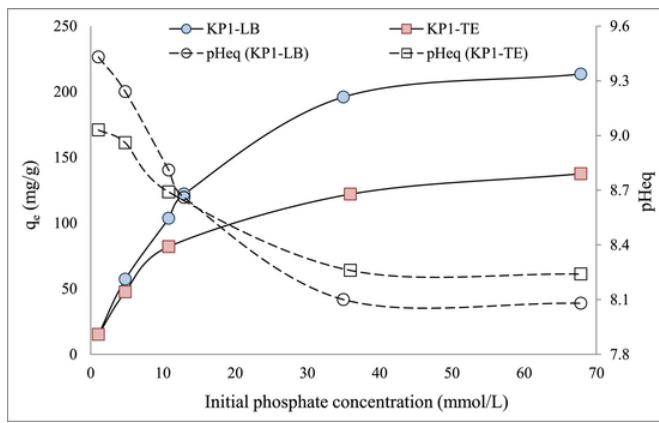


Fig. 6. The equilibrium pH variation as a function of initial phosphate concentration (initial pH 8) and the phosphate uptake as a function of equilibrium adsorbed concentration for KP1-LB and KP1-TE.

d) Formation of calcium phosphate minerals with Ca (II) occupying zeolite ion exchange sites:



From a thermodynamic point of view, the most favored reaction is the formation of Ca-phosphate (e.g., brushite or Hap) (Eqs. (12) and (13)) with the release of H^+ ions and the resulting decrease in the pH, as was shown for both zeolites to values below 8 (Hermassi et al., 2016b). XRD analysis of the loaded zeolites samples (Fig. 7), confirmed that from the two expected calcium phosphates minerals only brushite ($\text{CaHPO}_4 \cdot 2\text{H}_2\text{O}(\text{s})$) was identified (e.g., $\log K_{\text{so}} = -6.6$), Dorozhkin, 2012).

XRD analysis of KP1 samples after sorption experiments detected the presence of brushite for initial phosphate concentration above $1000 \text{ mgP-PO}_4/\text{L}$. However, the presence of Ca-phosphate minerals was not detected for low phosphate concentration levels (Fig. 7), it can be related to the formation of nanocrystals that could not be detected or the formation of amorphous structures. In general, precipitation associated with fast kinetics is accompanied by the reduction in the solids' crystallinity. For all the samples XRD patterns show the occurrence of

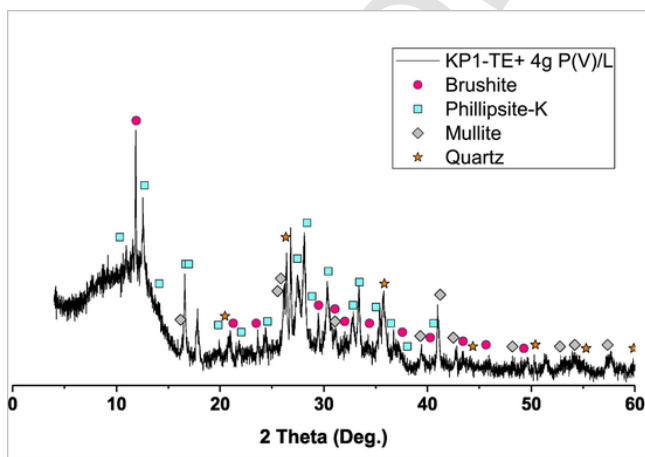


Fig. 7. XRD patterns (brushite, phillipsite-K/W zeolite, mullite and quartz) of the K-zeolitic product KP1-TE after phosphate sorption with an initial phosphate concentration of $4 \text{ gP-PO}_4/\text{L}$ at $\text{pH} = 8$.

brushite in addition to the W zeolite (or phillipsite) and relict phases from FA such mullite and quartz.

The phosphate sorption data are well described by Langmuir isotherm ($R^2 \geq 0.99$), while Freundlich isotherm ($R^2 \leq 0.94$) (Table 6 and Fig. 8) provides a good description only at the lower concentration ranges. Therefore, monolayer and homogenous sorption or and/ion exchange at specific and equal affinity sites available on the KP1-TE and KP1-LB surface is likely to occur. In fact, favourable phosphate sorption is revealed by the values of $0 < K_L < 1$ (Foo and Hameed, 2010), and the maximum phosphate sorption capacities along Langmuir isotherm were 250 ± 5 and $141 \pm 3 \text{ mgP-PO}_4/\text{g}$ for KP1-LB and KP1-TE, respectively (Table 6).

3.5. Scope for the application of K-zeolites as reactive sorbents for P recovery from WWTP

The P-sorption capacity shown by the synthesized Ca-bearing K-zeolites has been compared with previously reported capacities with inorganic sorbents. Blends of N and P containing loaded reactive sorbents with bio-solids from urban waste water are being proposed for soil enrichment from a sustainable perspective taking into account economic, agronomic and circularity criteria. Examples of initiatives to promote valorisation routes of nutrients from wastewater are summarized in Table 7.

Waste and by-products generated in power generation and in the processing industry (e.g., mining and metallurgical sludge, mine tailings, coal and biomass combustion fly ash) or inorganic based sorbents and bio-sorbents have been evaluated. The basis for the selection of the materials includes minerals with a high content of Mg or Ca (carbonates, silicates, oxides, or zeolites in Ca and Mg forms) to promote the release of Ca and Mg ions and then the stabilization of P (phosphate) as Ca-Mg phosphate minerals, or the use of metal oxides and hydroxides (Fe and Al) to promote P (phosphate) sorption through the Fe and Al surface groups ($> \text{MOH}$) or zeolites. In the case of ammonium and potassium cations, the main option has been the use of ion-exchange materials in Na, Ca and Mg. The most widely evaluated solution is the

Table 6
Langmuir and Freundlich isotherm parameters for KP1-LB and KP1-TE at pH 8.

Isotherms models/ adsorbent	Langmuir		Freundlich			
	q_m	K_L	R^2	K_F	n	R^2
KP1-LB	248.2 ± 5	0.0015	0.99	4.7	2.2	0.94
KP1-TE	140.8 ± 3	0.0048	0.99	6.1	2.6	0.84

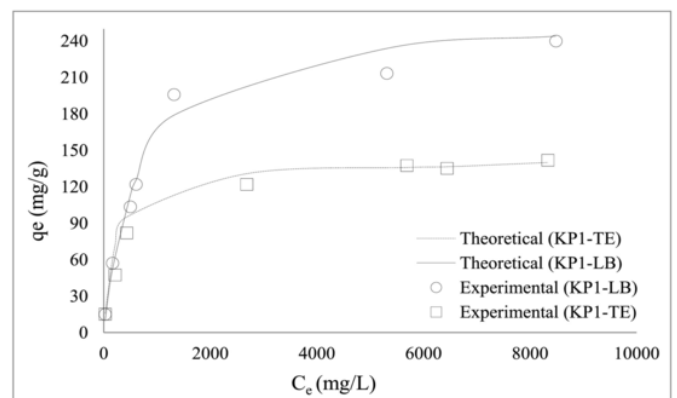


Fig. 8. Phosphate sorption isotherms at fixed pH 8 and predicted by the Langmuir model for KP1-TE and KP1-LB.

Table 7
Comparison of reported studies on the recovery of nutrients N and P from urban, industrial and farming wastewaters by using reactive materials.

Type of waste	Reactive materials used	Potential application	Recovered nutrient forms	Reference
Treated urban wastes water	Powdered Natural Zeolite modified with Fe, Al and Mn oxides (clinoptilolite)	The N-P loaded sorbents showed good nutrient bio-availability ratios as co-substrate for soil quality improvement	Ammonium exchanged onto ionogenic zeolite sites and phosphate sorbed on Fe/Al/Mn oxides sites	(Guaya et al., 2017, 2016, 2015)
Treated urban wastes water	Powdered Natural Zeolite converted to K-form and modified with Fe, Al and Mn oxides (clinoptilolite)	The N-P-K loaded sorbents showed good nutrient bio-availability ratios as co-substrate for soil quality improvement	Ammonium/potassium exchanged onto ionogenic zeolite sites and phosphate sorbed on Fe/Al/Mn Oxides sites	(Guaya et al., 2018)
Potassium-rich sludge anaerobic digestion side-streams	Powdered- 1-Na ⁺ -zeolite NaP1 2-Ca ²⁺ -zeolite CaP1 3-Caustic magnesia (Magna L)	The N-P-K-loaded sorbents showed good nutrient release and bioavailability ratios as co-substrates for soil quality improvement	Brushite Struvite k-Struvite	(Hermassi et al., 2017a)
Pig slurry	Commercial and industrial magnesium oxide by-products from magnesite calcination were blended with K ₂ HPO ₄	Study covered the reactivity of different magnesium by-products to promote ammonium recovery by struvite precipitation.	Bobierite Newberyite Struvite	(Romero-Güiza et al., 2015)
Treated wastewater effluents	A sodium zeolite synthesized from coal fly ash (NaP1-NA) was modified to calcium and magnesium forms (Ze-Ca, Ze-Mg)	Loaded zeolites, which contain ammonium and phosphate as well as calcium or magnesium, could be potentially used as slow-release inorganic fertilizer	Brushite Struvite.	(You et al., 2017)
Treated waste water	Two different types of Fly ashes from two coal power stations with different CaO(s) contents (Los Barrios (FA-LB (2.8% w)) and Teruel (FA-TE (4.8% w)))	Potential fertilizer, even in calcareous soils.	Brushite	(Hermassi et al., 2017b)

use of natural or synthetic zeolites produced from fly ash (Hermassi et al., 2016b). Alternative Romero-Güiza et al. (2014) proposed the use of MgHPO₄(s) as a precursor for the formation of struvite (NH₄MgPO₄·6H₂O(s)). The studies describing the applications where nutrients were recovered from both treated urban WWTP using natural zeolites modified with metal hydroxides for the simultaneous recovery of N and P are summarized in Table 7. As can be seen, the incorporation of K as a load-bearing sorbent is rarely reported and then the use of Ca-bearing K-zeolites as reactive sorbents could be a solution to improve the fertilizing contribution associated with potassium. Recently, a natural clinoptilolite was modified to K-form to balance the N-P-K ratio (Guaya et al., 2017; Hermassi et al., 2017a). The release performance of the N,P,K loaded zeolites shown suitable leaching rates in agronomical applications (Guaya et al., 2018). The recovery of P and N from anaerobic digestion side-streams was demonstrated by using mixtures of K-zeolites with MgO(s) by Hermassi et al. (2017a). Stabilization of N,P-K, was achieved by using the exchange position on the zeolitic materials and by formation of struvite and bobierite, both recognized as slow-release fertilizers.

According to the results of this study it has been demonstrated the capacity of Ca bearing K-zeolites to stabilize P, from waste water effluents, as Ca-phosphates mainly as brushite, taking advantage of the residual CaO(s) content on the fly-ash used for the synthesis of Merlinoite and/or W-zeolite.

It is worth to mention that the economic analyses of the use of slow-release fertilizers will determine the feasibility of being applied to agricultural systems. The specific sorbent-nutrient interactions and the nutrient release rate are both important properties to consider that were outside the scope of this study. Work in progress has been directed at improving the materials prepared when designing nutrient-loaded sorbent fertilizers properties: i) affinity for both cations and anions (NH₄⁺, K⁺, NO₃⁻, and HPO₄²⁻), ii) stability under soil environmental conditions, iii) slow-release characteristics, (iv) water-holding capacity, and (v) ability to function for long periods of time. The addition and use of nutrient-loaded sorbents improves agricultural yields and nutritional qualities of the soil, and those indicators will be used to analyse whether the materials can be applied at full-scale. The key issues that could promote circular approaches to valorise the nutrients from WWTP are the availability of feedstocks, the technology to recover and

apply the sorbents, the economic and financial viability throughout the supply chain and finally the regulatory framework that allows the circularity of the nutrients.

4. Conclusions

Merlinoite and W rich zeolitic products synthesized from FA-TE and FA-LB by KOH hydrothermal activation were found to have encouraging properties as a sorbent for phosphate from aqueous solution. Both Ca-bearing K-zeolites have been shown as suitable sorbents for phosphate recovery in the expected pH range (6 to 9) of wastewater effluents. The maximum phosphate sorption capacities measured were 250 ± 5 mgP-PO₄/g for KP1-LB, and 141 ± 3 mgPO₄/g for KP1-TE. The sorption process proceeds via a diffusion-controlled process involving phosphate ions within the K-FA particles coupled with CaO(s) dissolution from zeolitic products, which provides the Ca(II) ions required for brushite (CaHPO₄·2H₂O(s)) formation on the zeolite surface. This process is important because promotes the formation of more soluble phosphate mineral as brushite (logK_{so} = -6.6) and it avoids the formation of relatively insoluble Ca-phosphate minerals, such as hydroxypatite (logK_{so} = -51), which have more limited fertilizing properties. The use of phosphate-containing mineral-based sorbents as soil amendments may be advantageous when other agronomic benefits are expected, such as the provision of other plant nutrients or the enhancement of the soil moisture-holding capacity. Kinetic data revealed that although the removal process involved a complex mechanism, implying dissolution and formation of mineral phases, the rate limiting step of the sorption process is the intra-particle zeolite diffusion of phosphate ions. Times to equilibrium attainment are compatible with the use of the Ca-bearing K-zeolites in stirred reactors.

Furthermore, the results obtained in this study shows K-zeolitic products obtained from KOH hydrothermal activation from FA as a promising material for the recovery of P ions from treated urban wastewater resulting in a potential fertilizing material to be used in the restoration of degraded land. Such type of approach for the valuation of this residue, increasing its economic value while reducing environmental and economic costs of landfill could be understood as an example of waste to product example inside the initiatives of the circular economy.

CRedit authorship contribution statement

Mehrez Hermassi: Investigation, Writing - original draft. **Cesar Valderrama:** Writing - review & editing, Conceptualization. **Oriol Font:** Writing - review & editing, Conceptualization. **Natalia Moreno:** Writing - review & editing, Conceptualization. **Xavier Querol:** Writing - review & editing. **Narjès Harrouch Batis:** Writing - review & editing. **Jose Luis Cortina:** Supervision, Writing - review & editing, Conceptualization.

Uncited references

Declaration of competing interest

The authors declare that they have no known competing financial interests or personal relationships that could have appeared to influence the work reported in this paper.

Acknowledgments

This study has been supported by the Waste2Product project (CT-M2014-57302-R), the R2MIT project (CTM2017-85346-R) and the Exce-lencia Severo Ochoa Project (CEX2018-000794-S) financed by Ministry of Science and Innovation (MINECO, Spain) and the Catalan govern-ment (project ref. 2017SGR312). Aigües de Barcelona is acknowledged for waste waters supply from El Prat WWTP.

Appendix A. Supplementary data

Supplementary data to this article can be found online at <https://doi.org/10.1016/j.scitotenv.2020.139002>.

References

- Álvarez, J, Roca, M, Valderrama, C, Cortina, J L, 2018. A phosphorous flow analysis in Spain. *Sci. Total Environ.* 612, 995–1006.
- Amrhein, C, Haghnia, G H, Kim, T S, Mosher, P A, Gagajena, R C, Amanios, T, De La Torre, L, 1996. Synthesis and properties of zeolites from coal fly ash. *Environ. Sci. Technol.* 30, 735–742.
- Anjani, R K Gollakota, Volli, Vikranth, Shu, Chi-Min, 2019. Progressive utilisation prospects of coal fly ash: a review. *Sci. Total Environ.* 951–989.
- Balsamo, M, Di Natale, F, Erto, A, Lancia, A, Montagnaro, F, Santoro, L, 2010. Arsenate removal from synthetic wastewater by adsorption onto fly ash. *Desalination* 263, 58–63.
- Balsamo, M, Di Natale, F, Erto, A, Lancia, A, Montagnaro, F, Santoro, L, 2012. Reuse of coal combustion ash as sorbent: the effect of gasification treatments. *Combust. Sci. Technol.* 184, 956–965.
- Barca, C, Troesch, S, Meyer, D, Drissen, P, Andreis, Y, Chazarenc, F, 2013. Steel slag filters to upgrade phosphorus removal in constructed wetlands: two years of field experiments. *Environ. Sci. Technol.* 47, 549–556.
- Bautista, J M, Kim, H, Ahn, D H, Zhang, R, Oh, Y S, 2011. Changes in physicochemical properties and gaseous emissions of composting swine manure amended with alum and zeolite. *Korean J. Chem. Eng.* 28 (1), 189–194.
- Bruker AXS TOPAS V2.0, 2000. General Profile and Structure Analysis Software for Powder Diffraction Data. Bruker AXS, Karlsruhe, Germany.
- Buondonno, A, Grilli, E, Capra, G F, Glorioso, C, Langella, A, Leone, A P, Leone, N, Odierna, P, Vacca, S, Vigliotti, R C, 2013. Zeolitized tuffs in pedotechnique for the reclamation of abandoned quarries. A case study in the Campania region (Italy). *J. Environ. Manag.* 122, 25–30.
- Burger, J, Zipper, C, Angel, P, Evans, D, Eggerud, S, 2011. Reforestation guidelines for unused surface mined lands: development, application and adoption. 28th Annu. Meet. Am. Soc. Min. Reclam. 90–112.
- Cejka, J, 2005. Zeolites and Ordered Mesoporous Materials: Progress and Prospects. volume 157.
- Chen, J, Kong, H, Wu, D, Hu, Z, Wang, Z, Wang, Y, 2006. Removal of phosphate from aqueous solution by zeolite synthesized from fly ash. *J. Colloid Interface Sci.* 300, 491–497.
- Dorozhkin, S V, 2012. Self-setting calcium orthophosphate formulations: cements, concretes, pastes and putties. *Int. J. Mater. Chem.* 1, 1–48.
- European Commission Towards a circular economy URL https://ec.europa.eu/commission/priorities/jobs-growth-and-investment/towards-circular-economy_en2018
- Font, O, Moreno, N, Querol, X, Coca, P, 2009. Differential Behaviour of Combustion and Gasification Fly Ash From Puertollano Power Plants (Spain) for the Synthesis of Zeolites and Silica Extraction. 166. pp. 94–102.
- Foo, K Y, Hameed, B H, 2010. Insights into the Modeling of Adsorption Isotherm Systems. 156. pp. 2–10.
- Gholamhoseini, M, Ghalavand, A, Khodaei-Joghan, A, Dolatabadian, A, Zakikhani, H, Farmanbar, E, 2013. Zeolite-amended cattle manure effects on sunflower yield, seed quality, water use efficiency and nutrient leaching. *Soil Tillage Res.* 126, 193–202.
- Guaya, D, Valderrama, C, Farran, A, Armijos, C, Cortina, J L, 2015. Simultaneous phosphate and ammonium removal from aqueous solution by a hydrated aluminum oxide modified natural zeolite. *Chem. Eng. J.* 271, 204–213.
- Guaya, D, Hermassi, M, Valderrama, C, Farran, A, Cortina, J L, 2016. Recovery of ammonium and phosphate from treated urban wastewater by using potassium clinoptilolite impregnated hydrated metal oxides as N-P-K fertilizer. *J. Environ. Chem. Eng.* 4, 3519–3526.
- Guaya, D, Valderrama, C, Farran, A, Cortina, J L, 2017. Simultaneous nutrients (N,P) removal by using a hybrid inorganic sorbent impregnated with hydrated manganese oxide. *J. Environ. Chem. Eng.* 5, 1516–1525.
- Guaya, D, Valderrama, C, Farran, A, Sauras, T, Cortina, J L, 2018. Valorisation of N and P from waste water by using natural reactive hybrid sorbents: nutrients (N,P,K) release evaluation in amended soils by dynamic experiments. *Sci. Total Environ.* 612, 728–738.
- Hermassi, M, Valderrama, C, Dosta, J, Cortina, J L, Batis, N H, 2015. Evaluation of hydroxyapatite crystallization in a batch reactor for the valorization of alkaline phosphate concentrates from wastewater treatment plants using calcium chloride. *Chem. Eng. J.* 267, 142–152.
- Hermassi, Mehrez, Valderrama, C, Gibert, O, Moreno, N, Font, O, Querol, X, Batis, N, Cortina, J L, 2016. Integration of powdered Ca-activated zeolites in a hybrid sorption-membrane ultrafiltration process (PAZ-UF) for phosphate recovery. *Ind. Eng. Chem. Res.* 55, 6204–6212.
- Hermassi, Mehrez, Valderrama, C, Moreno, N, Font, O, Querol, X, Batis, N H, Cortina, J L, 2016. Powdered Ca-activated zeolite for phosphate removal from treated waste-water. *J. Chem. Technol. Biotechnol.* 91, 1962–1971.
- Hermassi, M, Valderrama, C, Gibert, O, Moreno, N, Querol, X, Batis, N H, Cortina, J L, 2017. Recovery of nutrients (N-P-K) from potassium-rich sludge anaerobic digestion side-streams by integration of a hybrid sorption-membrane ultra filtration process: use of powder reactive sorbents as nutrient carriers. *Sci. Total Environ.* 599–600, 422–430.
- Hermassi, M, Valderrama, C, Moreno, N, Font, O, Querol, X, Batis, N H, Cortina, J L, 2017. Fly ash as reactive sorbent for phosphate removal from treated waste water as a potential slow release fertilizer. *J. Environ. Chem. Eng.* 5, 160–169.
- Hillier, S, 2000. Accurate quantitative analysis of clay and other minerals in sandstones by XRD: comparison of a Rietveld and a reference intensity ratio (RIR) method and the importance of sample preparation. *Clay Miner.* 35, 291–302.
- Holler, H, Wirsching, U, 1985. Zeolite Formation From Fly-Ash. *Fortschritte Der Mineral.* 63. pp. 21–43.
- Hubbard, C R, Snyder, R L, 1988. RIR - measurement and use in quantitative XRD. *Power Diff.* 3, 74–77 ICDD database. <http://www.icdd.com/pdf-2/>.
- International Energy Agency (IEA) Tracking industry IEA Paris <https://www.iea.org/reports/tracking-industry2019>
- Itskos, G, Koukouzas, N, Vasilatos, C, Megremi, I, Moutsatsou, A, 2010. Comparative uptake study of toxic elements from aqueous media by the different particle-size-fractions of fly ash. *J. Hazard. Mater.* 183, 787–792.
- Kitson, R E, Mellon, M, 1944. Colorimetric determination of phosphorus as molybdovanadophosphoric acid. *Ind. Eng. Chem. Anal.* 16 (6), 379–383.
- Larney, F J, Angers, D A, 2012. The role of organic amendments in soil reclamation: a review. *Can. J. Soil Sci.* 92, 19–38.
- Li, J, Zhuang, X, Font, O, Moreno, N, Vallejo, V R, Querol, X, Tobias, A, 2014. Synthesis of merlinoite from Chinese coal fly ashes and its potential utilization as slow release K-fertilizer. *J. Hazard. Mater.* 265, 242–252.
- Liberti, L, Passino, R, 1977. In: Marinsky, J A, Y.M. (Eds.), *Ion Exchange and Solvent Extraction*. Marcel Dekker, Inc, New York, p. 7.
- Moreno, N, Querol, X, Ayora, C, Ferna, C, Pereira, ÁN, Janssen-jurkovicova, M, 2001. Utilization of Zeolites Synthesized From Coal Fly Ash for the Purification of Acid Mine Waters. 35. pp. 3526–3534.
- Moreno, N, Querol, X, Andres, M, Janssen, M, Nugteren, H, 2002. Pure Zeolite Synthesis From Silica Extracted From Coal Fly Ashes + 279. pp. 6–8.
- Murayama, N, Yamamoto, H, Shibata, J, 2002. Zeolite synthesis from coal fly ash by hydrothermal reaction using various alkali sources. *J. Chem. Technol. Biotechnol.* 77, 280–286.
- Murayama, N, Yamamoto, H, Shibata, J, 2002. Mechanism of zeolite synthesis from coal fly ash by alkali hydrothermal reaction. *Int. J. Miner. Process.* 64, 1–17.
- Murayama, N, Takahashi, T, Shuku, K, Lee, H ho, Shibata, J, 2008. Effect of reaction temperature on hydrothermal syntheses of potassium type zeolites from coal fly ash. *Int. J. Miner. Process.* 87, 129–133.
- Nissen, L R, Lepp, N W, Edwards, R, 2000. Synthetic zeolites as amendments for sewage sludge-based compost. *Chemosphere* 41, 265–269.
- Pramatha, P, Prabir, D, 2003. Zeolites: a primer. In: *Handbook of Zeolite Science and Technology*, 1st edition Taylor and Francis Group, pp. 1–24 Chapté 1.
- Querol, Umana, J, Plana, F, Alastuey, A, Lopez-Soler, A, Medinaceli, A, A.V, 1995. The Rietveld method. In: Young, R A (Ed.), *International Union of Crystallography*. Oxford University Press, p. 308 9780198559122.
- Querol, X, Plana, F, Alastuey, A, López-Soler, A, 1997. Synthesis of Na-zeolites from fly ash. *Fuel* 76, 793–799.
- Querol, X, Alastuey, A, Moreno, N, Alvarez-Ayuso, E, García-Sánchez, A, Cama, J, Ayora, C, S., M, 2006. Immobilization of heavy metals in polluted soils by the addition of zeolitic material synthesized from coal fly ash. *Chemosphere* 62, 171–180.

- Rayalu, S, Meshram, S U, Hasan, M Z, 2000. Highly Crystalline Faujasitic Zeolites From Flyash. pp. 123–131.
- Rayalu, S S, Udhoji, J S, Munshi, K N, Hasan, M Z, 2001. Highly Crystalline Zeolite — A From Flyash of Bituminous and Lignite Coal Combustion. 88. pp. 107–121.
- Romero-Güiza, M S, Astals, S, Chimenos, J M, Martínez, M, B, J M-A, 2014. Improving anaerobic digestion of pig manure by adding in the same reactor a stabilizing agent formulated with low-grade magnesium oxide. *Biomass Bioenergy* 67, 243–251 ScienceDirect.
- Romero-Güiza, M S, Astals, S, Mata-alvarez, J, Chimenos, J M, 2015. Feasibility of coupling anaerobic digestion and struvite precipitation in the same reactor: evaluation of different magnesium sources. *Chem. Eng. J.* 270, 542–548.
- Valderrama, C, Barios, J I, Caetano, M, Farran, A, Cortina, J L, 2010. Kinetic evaluation of phenol/aniline mixtures adsorption from aqueous solutions onto activated carbon and hypercrosslinked polymeric resin (MN200). *React. Funct. Polym.* 70, 142–150.
- Vallejo, V R, Allen, E B, Aronson, J, Pausas, J G, Cortina, J, Gutierrez, J R, 2012. Restoration of Mediterranean-type woodlands and shrublands. *Restor. Ecol. New Front.* 130–144.
- Villaseñor, J, Rodríguez, L, Fernández, F J, 2011. Composting domestic sewage sludge with natural zeolites in a rotary drum reactor. *Bioresour. Technol.* 102, 1447–1454.
- Walker, G M, Weatherley, L R, 1999. Kinetics of Acid Dye Adsorption on gac 33.
- Wang, Qiang, Song, Xiaoxin, Liu, Yi, 2020. China's coal consumption in a globalizing world: insights from multiregional input-output and structural decomposition analysis. *Sci. Total Environ.* 711, 134790.
- Watanabe, Y, Yamada, H, Ikoma, T, Tanaka, J, Stevens, G W, Komatsu, Y, 2014. Preparation of a zeolite NaP1/hydroxyapatite nanocomposite and study of its behavior as inorganic fertilizer. *J. Chem. Technol. Biotechnol.* 89, 963–968.
- Wendling, L A, Blomberg, P, Sarlin, T, Priha, O, Arnold, M, 2013. Phosphorus sorption and recovery using mineral-based materials: sorption mechanisms and potential phytoavailability. *Appl. Geochem.* 37, 157–169.
- de Woolf, P M, Visser, J W, 1988. Absolute intensities - outline of a recommended practice. *Powder Diffract.* 3, 202–204.
- You, X, Valderrama, C, Cortina, J L, 2017. Simultaneous recovery of ammonium and phosphate from simulated treated wastewater effluents by activated calcium and magnesium zeolites. *Chem. Technol. Biotechnol.* 92 (9), 2400–2409.
- Young, R A, 1995. The Rietveld Method. International Union of Crystallography. Oxford University Press, 9780198559122 308 p..
- Zeng, R, Umana, J C, Querol, X, Lopez-Soler, A, Plana, F, Zhuang, X, 2002. Zeolite synthesis from a high Si-Al fly ash from East China. *J. Chem. Technol. Biotechnol.* 77, 267–273.
- Zhang, B hua, Wu, D yi, Wang, C, He, S bing, Zhang, Z jia, Kong, H nan, 2007. Simultaneous removal of ammonium and phosphate by zeolite synthesized from coal fly ash as influenced by acid treatment. *J. Environ. Sci.* 19, 540–545.
- Zorpas, A A, Kapetanios, E, Zorpas, G A, Karlis, P, Vlyssides, A, Haralambous, I, Loizidou, M, 2000. Compost produced from organic fraction of municipal solid waste, primary stabilized sewage sludge and natural zeolite. *J. Hazard. Mater.* 77, 149–159.
- Zwingmann, N, Mackinnon, I D R, Gilkes, R J, 2011. Use of a zeolite synthesised from alkali treated kaolin as a K fertiliser: glasshouse experiments on leaching and uptake of K by wheat plants in sandy soil. *Appl. Clay Sci.* 53, 684–690.